Acta Geochim (2020) 39(2):172–180
https://doi.org/10.1007/s11631-020-00395-6

ORIGINAL ARTICLE

The effect of pH on the sorption of gold nanoparticles on illite

Yuhong Fu[1] · Quan Wan[2,3] · Zonghua Qin[2] · Xin Nie[2] · Wenbin Yu[2] · Shanshan Li[4]

Received: 21 December 2019 / Revised: 29 December 2019 / Accepted: 2 January 2020 / Published online: 18 January 2020

Abstract Sorption between nanoparticles (NPs) and minerals may critically affect the migration of associated elements as well as the environmental impact of NPs. Since illite is widely present in soil, sediment, and water, we have experimentally investigated the sorption behavior of citrate-coated gold nanoparticles (AuNPs) as model NPs on illite under different pH and mineral mass conditions. We demonstrated that sorption of these negatively charged AuNPs strongly depended on the suspension pH. At pH above 8, which coincided with the apparent point of zero charge (pH 7.9) of our illite sample, only marginal sorption of AuNPs was observed. At pH 3–8, significant sorption of AuNPs on illite was found, with almost complete sorption occurring at more acidic conditions (pH 3–4). TEM observations revealed that sorption took place through the attachment AuNPs on illite edges. At pH 2, AuNPs mostly formed chain-like fused structures and precipitated out of the suspension. Based upon the above pH dependence, residual organic ligand content after sorption, and complementary sorption results with positively charged AuNPs, we conclude that the sorption process is mainly driven by the electrostatic attraction between negatively charged AuNPs and positively charged illite edges, with possible competitive involvement of citrate molecules. We expect that our findings will improve our understanding of NP–mineral interaction and the environmental fate of NPs.

Keywords Gold nanoparticles · Illite · Sorption · Charge · Electrostatic interaction

✉ Quan Wan
wanquan@vip.gyig.ac.cn

Yuhong Fu
fuyuhong10@163.com

Zonghua Qin
qinzonghua@mail.gyig.ac.cn

Xin Nie
niexin@mail.gyig.ac.cn

Wenbin Yu
yuwenbin@mail.gyig.ac.cn

Shanshan Li
Lss8132@163.com

[1] School of Geographic and Environmental Sciences, Guizhou Normal University, Guiyang 550025, Guizhou, China

[2] State Key Laboratory of Ore Deposit Geochemistry, Institute of Geochemistry, Chinese Academy of Sciences, Guiyang 550081, Guizhou, China

[3] CAS Center for Excellence in Comparative Planetology, Hefei 230026, Anhui, China

[4] School of Chemistry and Materials Science, Guizhou Normal University, Guiyang 550025, Guizhou, China

1 Introduction

Nanoparticles (NPs), including both natural nanoparticles (NNPs) and engineered nanoparticles (ENPs), are ubiquitous in the environment. In all spheres of the Earth, NNPs can be generated through a variety of thermal, mechanical, chemical, photochemical, or biological processes (Sharma et al. 2015). By estimation, thousands of terragrams ($\sim 10^{15}$ g) of NNPs are produced each year by just biogeochemical processes alone (Barnard and Guo 2012). Moreover, as ENPs have rapidly expanded in commercial applications, the global market value of ENPs is expected to increase from 12.7 billion USD (in 2008) to approximately 30 billion USD (in 2020) (Wang et al. 2013), and the production of ENPs has reached approximately 350,000 tonnes in 2016 (Goswami et al. 2017). At any stage of their

life cycle (i.e. manufacturing, transportation, usage, disposal, or recycling), a considerable amount of ENPs may be intentionally or accidentally released into the environment, including soils, water bodies, and the atmosphere (Keller et al. 2013). It is expected that such large quantities of NNPs and ENPs in nature will play a substantial role in the geochemical migration, cycling, and distribution of associated elements, which may consequently pose potential threats to the environment and human health (Keller et al. 2013; Peralta-Videa et al. 2011; Sharma et al. 2015; Wagner et al. 2014). To assess the unique geochemical and environmental impact of NPs, it is necessary to examine not only the NPs' potential toxicity but also their fate and transport in the environment (Wiesner et al. 2006).

NP sorption on mineral surfaces commonly occurs in aquatic environments and is one of the most important processes determining the fate, transport, and environmental risk of NPs. Because interactions between NPs and minerals are complicated by many features of NPs and minerals (e.g. size, shape, structure, surface coating etc.) (Fu et al. 2017; Luo et al. 2018), classical colloidal science based on Derjaguin–Landau–Verwey–Overbeek (DLVO) theory often fails to adequately describe NP behaviors (Hotze et al. 2010; Monfared et al. 2018). Therefore, many recent scientific endeavors have aimed at filling this important knowledge gap via experimental approaches. Since clay is abundantly present in soil, water, and air, heteroaggregation (i.e., sorption) between NPs and clay minerals is considered a likely process and has attracted much attention. For example, Zhou et al. investigated the effects of ionic strength (IS) on the sorption of Ag or TiO_2 NPs on montmorillonite at pH 4 and 8 (Zhou et al. 2012). Wang et al. studied the effect of kaolin on the aggregation of Ag and TiO_2 NPs under different pH (also at 4 and 8), IS and natural organic matter (NOM) conditions (Wang et al. 2015). Kim et al. discussed the effect of kaolinite on the transport of polymer-stabilized zero-valent iron NPs in heterogeneous porous media at pH 6–8 (Kim et al. 2012). Guo et al. conducted packed column experiments to study the transport behavior of TiO_2 NPs with montmorillonite or diatomite in the presence of NaH_2PO_4 solution (Guo et al. 2018). Gupta et al. studied the electrostatic interaction between ZnO NPs and montmorillonite and found the enhanced toxicity of ZnO NP–clay heteroagglomerates in *Tetrahymena pyriformis* (Gupta et al. 2017). These studies demonstrated that the interaction and sorption between clay minerals and NPs can be quite complex, which highly depend upon the properties of various tested materials and could to various extents be sensitive to external conditions.

Gold nanoparticles (AuNPs) are well known for both their ancient usages and their versatility in many modern fields, including catalysis, medical diagnosis, chemical sensing, etc. (Daniel and Astruc 2004). Despite widespread applications, some experimental studies have raised serious health and safety concerns regarding the cytotoxicity of AuNPs. For example, the reduced viability of human cells (e.g., sperm cells and dermal fibroblasts) and certain damage to their activities were indicated upon exposure to AuNPs (Pernodet et al. 2006; Wiwanitkit et al. 2009). To evaluate the transport, fate, and related exposure pathways of AuNPs in the environment, it is important to obtain a solid understanding of AuNP–mineral sorption behavior. Interestingly, AuNPs are also found in nature, for example, in a number of hypogene and supergene ore deposits, where (especially in weathering-related deposits) AuNPs might be found at the rim of clay particles (Hong et al. 1999; Hough et al. 2011; Palenik et al. 2004). In such cases, the AuNP–clay interactions may constitute a key step in the mineralization process.

However, most studies involving AuNP–clay mineral interactions seem to focus on improving properties and thus broadening applications of AuNP-based materials. For example, several AuNP–clay hybrid materials were prepared for the purpose of enhancing material properties and functionalities (e.g., thermal stability, catalytic, and biosensing abilities) (Belova et al. 2008; Hata et al. 2007; Paek et al. 2006; Varadwaj and Parida 2013; Zhao et al. 2008). To the best of our knowledge, there is still a lack of systematic studies on the sorption behavior of AuNPs on clay minerals. Therefore, we have recently conducted an experimental study aimed at determining how clay minerals (such as illite) interact with AuNPs and thus influence the fate and exposure route of AuNPs in an aqueous environment. The reason for choosing the AuNP–illite system is partly because illite comprises more than half of the total clay minerals in the Earth's crust (Gradusov 1974). Nevertheless, the interfacial properties of illite have not been thoroughly studied (Du et al. 1997; Gu and Evans 2007; Kriaa et al. 2009). In this paper, we report our experimental results revealing the dominant role of pH in the sorption of AuNPs on illite, and systematically discuss the sorption mechanism. The findings contribute to understanding the interaction between NPs and mineral surfaces and the potential fate and toxicity of NPs under aquatic environments.

2 Materials and methods

2.1 AuNPs and illite

Negatively charged AuNPs were synthesized using the classic Frens method (Frens 1973). Briefly, 300 mL of chloroauric acid solution ($HAuCl_4$, 0.01%, w/w) was heated to boiling under reflux and vigorous magnetic stirring. Thereafter, 10.5 mL of a freshly prepared sodium

citrate solution (1%, w/w) was quickly added to the boiling solution and stirred for 15 min. The initial molar ratio of citrate/$HAuCl_4$ was 4.65, and a wine-red colloid was obtained and cooled down to ambient temperature. Positively charged AuNPs [hereinafter referred to as AuNPs(+)] were synthesized using a seed-mediated method (Luo et al. 2018; Sau and Murphy 2004; Wang et al. 2008) to further study the sorption mechanism. Illite sample was collected from Jinsha, Guizhou Province, China and was cleaned in deionized water.

2.2 Characterization of materials

The size and morphology of the prepared AuNPs were characterized using a transmission electron microscope (TEM; JEM-2000FXII, JEOL, Japan) operated at 160 kV. Particle size analysis was performed using ImageJ (US National Institutes of Health) software. The adsorption spectrum of the Au colloid was recorded in a UV–Vis spectrophotometer (Cary 300, Agilent Technologies, USA). The mineral composition of illite was estimated by X-ray diffraction (XRD; D/Max-2200, Rigaku, Japan). The Brunauer–Emmett–Teller (BET) specific surface area of illite was determined by nitrogen adsorption measurements at 77 K (Autosorb-iQ2-MP, Quantachrome, USA). The grain size of the illite was measured using a particle size analyzer (LS 13 320, Beckman Coulter, USA).

2.3 Sorption experiments

The sorption of AuNPs on illite was studied by batch experiments. The sorption experiments were repeated at least twice. Each sorption system contained different masses of illite (0.07, 0.1, and 1 g) in 20 mL of gold colloid ($\sim$ 57 mg/L), with its initial pH adjusted from 2 to 10 by adding a small amount of HCl or NaOH solution of the appropriate concentration. After 6 days of shaking at 25 °C, illite was separated by centrifugation (220 g, 30 min), and 2 or 5 mL of the supernatants was digested (1 mL aqua regia, overnight) for analysis of Au using a flame atomic absorption spectrophotometer (AAS; 990 SUPER, Persee, China). The concentration of citrate in the supernatants was determined by high-performance liquid chromatography (HPLC; Agilent 1100, Agilent Technologies, USA). HPLC was equipped with a multiple wavelength detector (MWD, was set at 215 nm) and a Zorbax SB-aq (3 × 100 mm, 1.8 μm) (Agilent) column. H_3PO_4 (0.1%, v/v) was used as the mobile phase in a constant flow of 0.6 mL/min and the column temperature was 40 °C. Furthermore, illite-free Au colloids were used as control samples, and the Au concentration was determined after shaking at 25 °C for the same period of time. To conveniently collect specimens for TEM observations, a series of sorption experiments were performed in a "static" manner (i.e., without shaking or stirring). After standing for 6 days, a small fraction of the upper-layer solid ("static" sample) was taken for TEM observations. To better understand the adsorption mechanism, sorption experiments between 0.1 g illite and AuNPs(+) were carried out at pH $\sim$ 4 and $\sim$ 9 using the same experimental procedure.

2.4 Potentiometric titrations

The apparent point of zero charge (PZC) of illite was determined using an automatic potentiometric titrator (T50, Mettler Toledo, Switzerland) with a glass electrode (DGi111-SC, Mettler Toledo). A suspension of illite (0.75 g) in 150 mL of deionized water was prepared and shaken for 6 days at 25 °C. Afterward, argon was bubbled into the suspension until the pH was stable. Fifty milliliters of the above suspension was added to a vessel purged with argon and immersed in a thermostat water bath at 25 °C. After equilibration, 1 mL of HNO_3 (0.5%, v/v) was added to the suspension, and the pH was lowered to approximately 3. The suspension was then slowly titrated up to pH 11 with 0.05 M NaOH, with each titration step allowed to stabilize until the drift of the measured potential was less than 0.04 mV/min. A similar titration was performed on the supernatant (as the blank) obtained by centrifugation of the suspension (18705 g, 10 °C, 30 min).

3 Results and discussion

3.1 Morphology and composition analysis

The as-synthesized gold sol showed a wine-red color with a UV–Vis absorbance peak at 519 nm and could remain stable against aggregation for up to 1 year under ambient conditions. Based on TEM analysis of more than 100 particles (Fig. 1), our synthesized AuNPs were monodispersed spherical particles with a mean diameter of 16.6 nm and a relative standard deviation (RSD) of 7.1%. The analysis of the XRD pattern (Fig. 2) indicated that our clay sample was composed of mostly illite (88.3%) in addition to a small amount of montmorillonite (6.2%), kaolinite (3.1%), amphibole (1.3%), and iron-containing minerals (1.1%). The BET surface area of illite was determined to be 15.0 m^2/g, and the average grain size was 25.9 μm.

3.2 Sorption experiments

3.2.1 Change in Au concentration

After sorption, a supernatant obtained via centrifugation was measured for its gold concentration. The Au

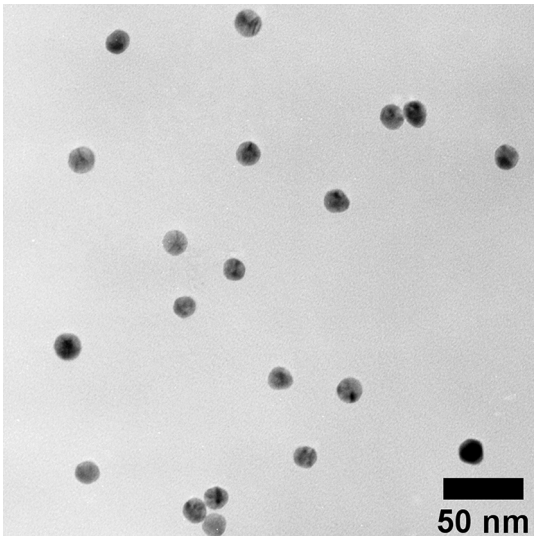

Fig. 1 TEM image of the AuNPs. Scale bar: 50 nm

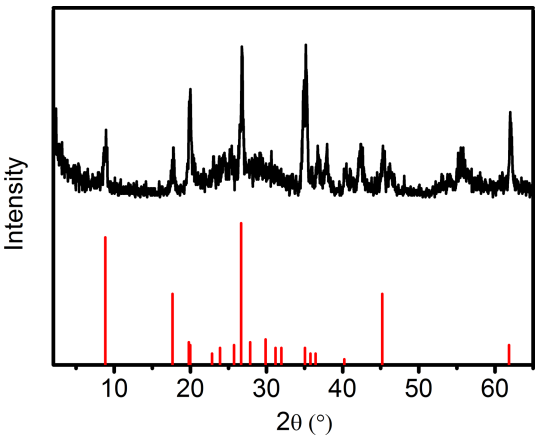

Fig. 2 XRD patterns of the illite sample (above) and illite reference (below, JCPDS No. 26-0911)

Table 1 Gold concentration after vibration in illite free control experiments

Initial pH	Au[a] (mg/L)
2.01	45.7
3.00	52.2
3.95	53.6
4.83	56.3
6.96	56.7
9.96	57.4

[a]Concentration of gold of control samples after stirring

concentration results presented in Fig. 3 reveal an apparent pH dependence of Au sorption on illite. We first analyzed the 0.1 g series samples. For samples with an initial pH $\leq$ 3.5, the originally wine red color of the gold colloids turned colorless very quickly, normally within 20 min

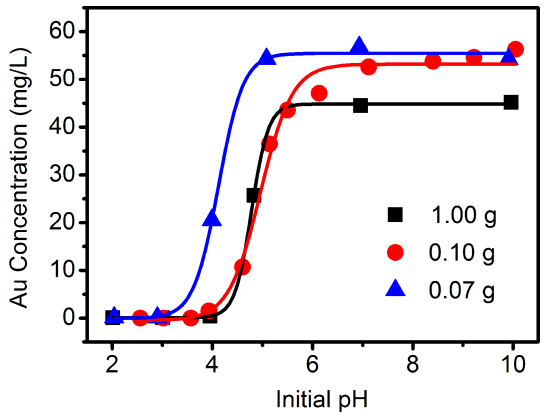

Fig. 3 Concentration of gold after sorption as a function of the initial pH

upon mixing with illite. It took 5–7 h for the sample with initial pH $\sim$ 4 to become colorless. AAS measurements indicated a gold concentration of nearly 0 for the colorless supernatants (pH $<$ 4), which was equivalent to complete ($\sim$ 100%) Au uptake. At an initial pH between 4 and 8, a partial diminishing of the wine red color was observed after days of mixing, and the sorption of Au decreased with increasing pH. At pH $>$ 8, the concentration of gold after sorption was similar to that of the original colloid, indicating negligible Au sorption.

For the illite-free control samples, the Au concentration (Table 1) decreased with decreasing pH after days of shaking, and a small amount of black agglomerates were observed at pH 2 and 3. The reduced stability of the Au colloids at lower pH was due to partial neutralization of negatively charged citrate ligand, which consequently lowered the electrostatic repulsion between AuNPs (Basu et al. 2007; Liu et al. 2012). However, the Au concentration change in the illite-free control samples was quite small compared with its original level (56–57 mg/L). The much larger pH dependence of Au sorption on illite could be attributed to the interaction between illite and AuNPs.

To evaluate the effect of the illite mass, sorption experiments with different amounts of illite (0.07 g and 1.00 g) were also carried out. Although fewer data points were collected for each of the 0.07 g and 1.00 g mass series (Fig. 3), the overall trend of Au concentration change with respect to pH was clearly very similar to that of the 0.1 g series, reinforcing the dominant role of pH in the sorption process. At pH $<$ 4, almost all Au was removed from the supernatant of the samples for all mass series. At higher pH, the Au concentration change seems to satisfactorily reflect the quite understandable recognition that more mass of adsorbent tends to adsorb more amount of adsorbate.

3.2.2 TEM observation

Several sampling protocols were used for TEM study, including taking samples directly from the sorption suspensions, from sediments after centrifugation, or from the solid interlayers in the "static" experiments described earlier. Through comparison, we found that the "static" samples appeared more suitable for TEM observation because the upper-layer illite adequately interacted with the AuNPs and interlayer specimens reasonably represented the microscopic characteristics of all sorption samples despite different sampling protocols. Notably, no significant differences were found between the pH dependence patterns of Au concentration in sorption experiments with or without shaking. Figure 4 shows representative TEM images of the interlayer illite in static samples, which illustrate the different states of AuNPs after the sorption experiment, including adsorbed (Fig. 4c, d), aggregated or fused (Fig. 4a), and free (Fig. 4f) AuNPs. At pH 2, AuNPs mostly formed chain-like fused structures, similar to the sponge-like Au aggregates reported by Zhang et al. (2014), and almost no adsorption of AuNPs on illite was observed (Fig. 4a, b). Such firmly aggregated Au chains should precipitate easily from the Au colloid, consistent with the rapid drop of Au concentration to 0. At pH 3–4, although some fusion of AuNPs could be found, the nearly complete sorption of Au was mostly due to the attachment of AuNPs at illite edges (Fig. 4c, d). When the pH increased in the range of 4–8, the illite edge–AuNP attachment was less frequently found (Fig. 4e). At pH > 8 (e.g., Fig. 4f), the AuNPs shown in the image were mostly due to evaporation of the Au colloid, and almost no adsorption between illite and AuNPs was observed, which was consistent with the change of Au concentration measurement again.

3.3 Mechanistic investigation

In understanding the sorption behavior of NPs on mineral surfaces, immense complexity is often encountered not only because of the inevitable multiplicity of chemical species, processes and phases in the system but also because of the elusive aspects of the nanosize-dependent interfacial properties. To understand the mechanism of pH-dependent adsorption, we determined the surface charge of illite, carried out additional sorption experiments of AuNPs(+), and analyzed the role of organic ligands in the AuNP–illite sorption.

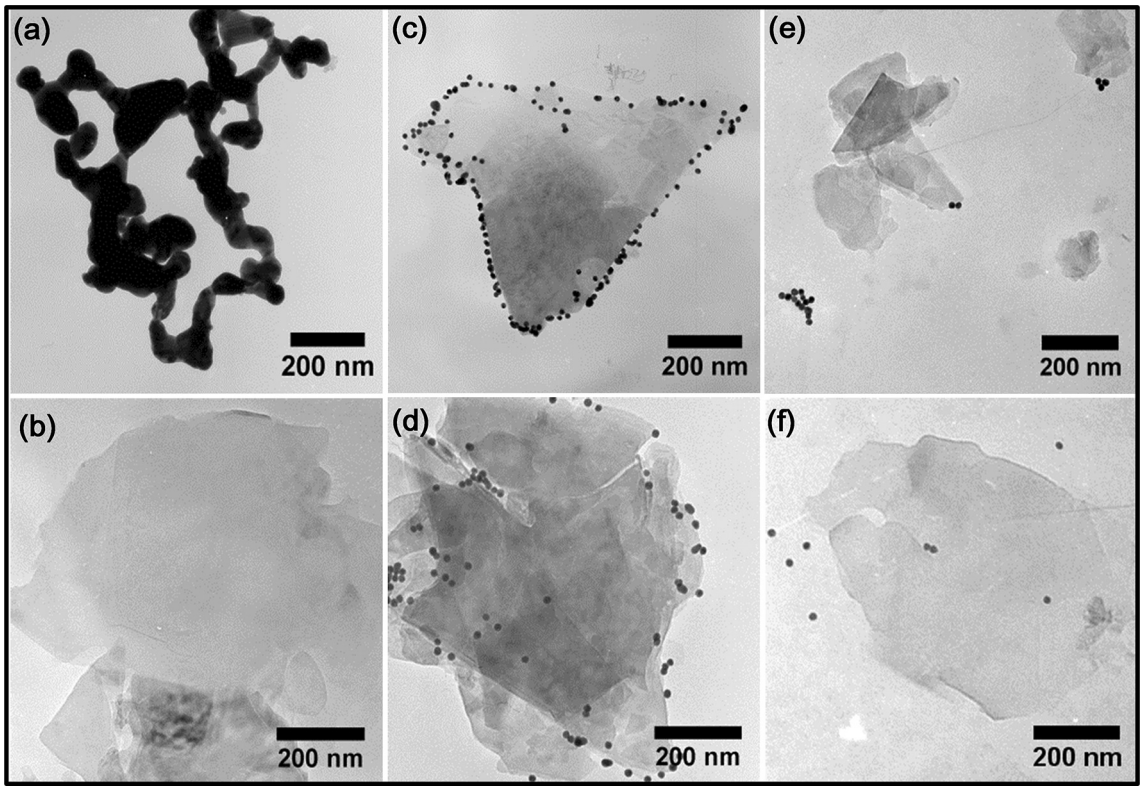

Fig. 4 TEM micrographs of the interlayer of "static" samples from the AuNP sorption experiments at **a** and **b** initial pH 2.01, **c** initial pH 3.00, **d** initial pH 3.95, **e** initial pH 4.83, and **f** initial pH 9.96. Scale bars: 200 nm

3.3.1 Surface charge of illite

Illite is a 2:1 type clay mineral with its unit layer consisting of one octahedral alumina sheet sandwiched between two tetrahedral silica sheets. Illite carries two types of surface charges, permanent negative charges (on basal planes) resulting from isomorphous substitution and pH-dependent charges due to protonation or deprotonation of hydroxyl groups ($\equiv$SiOH, $\equiv$AlOH) at the edge surfaces (Liu et al. 2013). The PZC defines a critical state at which the charge density on a surface is zero, and for oxides, the PZC is usually determined as the pH value at the common intersection point (CIP) of the acid–base titration curves at different ionic strengths (Kraepiel et al. 1998). Unlike oxides, minerals with permanent charges do not have a CIP of titration lines under different IS values, and in fact, their PZCs vary with the IS. For clay minerals (including illite) with permanent negative charge, the PZCs usually increase with a decrease in the IS (Avena et al. 2003; Delhorme et al. 2010; Gu and Evans 2007; Kraepiel et al. 1998).

We used a back-titration technique to evaluate the PZC of our illite sample. To minimize the influence of the IS and other solution parameters, the condition (including the mixing time and solid/liquid ratio, etc.) for preparing the titration, suspension was maintained to be very similar to that of the sorption samples. The supernatant of the titration suspension without any acid or base addition was used as the blank (Schulthess and Sparks 1986). As shown in Fig. 5, the titration curves intersect at pH 7.9, which suggests an apparent PZC of illite at this pH. At pH $<$ 7.9, the protonation of hydroxyl groups (mostly aluminol) at the edge surfaces of our illite should dominate, and correspondingly, the overall sample carries a positive charge. At pH $>$ 7.9, the illite sample carries negative charges due to deprotonation of the silanol and aluminol groups.

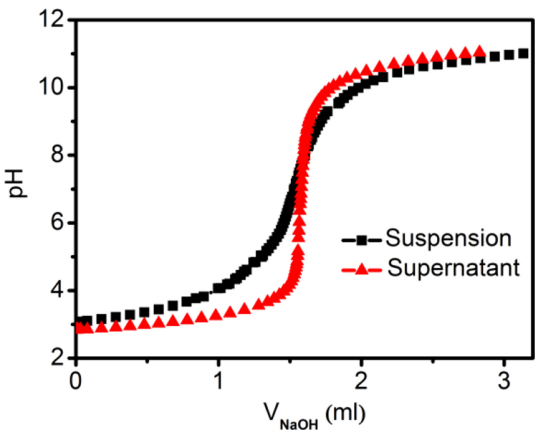

Fig. 5 Potentiometric titration curves of the illite suspension and corresponding supernatant

3.3.2 Sorption of AuNPs(+) on illite

To obtain a more comprehensive understanding of the sorption mechanism, we used positively charged AuNPs(+) (11.34 mg/L) for sorption at pH $\sim$ 4 and pH $\sim$ 9, respectively. Table 2 presents the relative residual concentration of the AuNPs(+) in the supernatants at different pH values. In contrast to the negatively charged AuNPs, AuNPs(+) could be strongly adsorbed by illite under both acidic and alkaline conditions, with nearly complete sorption occurring at pH $\sim$ 9 only. The AuNPs(+)–illite sorption samples were also characterized by TEM observations (Fig. 6). Unlike the dominant edge sorption of negatively charged AuNPs, most AuNPs(+) were adsorbed on the negatively charged basal planes at both pH values. Nevertheless, more edge adsorption can be found from the sample at pH $\sim$ 9 than that at pH $\sim$ 4.

3.3.3 Adsorption of citrate on illite

Residual organic ligands from NP synthesis may fundamentally influence the interfacial interaction between the NP and mineral surface and thus enable the remarkable control of the NP–mineral sorption behavior (Wagener et al. 2012). Functioning as a reducing and stabilizing agent, a considerable amount of citrate (292–300 mg/L) exists in our gold colloids prepared by the Frens method (with citrate/$HAuCl_4$ molar ratio: 4.65). We measured the concentrations of citrate in gold colloid samples before and after sorption with illite (0.1 g) using HPLC. While the initial citrate concentration did not vary much with pH, the concentration of citrate after sorption significantly changed with pH (Fig. 7). Considering the possible contribution from the adsorption or desorption of citrate on AuNP is quite small (i.e., a maximal surface density of 3 citrate per nm^2 on an AuNP corresponds to a bulk citrate concentration $<$ 2 mg/L) (Nichols et al. 2004; Park and Shumaker-Parry 2014; Rostek et al. 2011), we attribute the decrease in the citrate concentration mainly to the adsorption of citrate on illite. At pH values outside 3–8, there was almost no adsorption of citrate, and the maximum adsorption occurred at pH 5.1. Similar pH dependence of citrate adsorption to clay minerals (including illite) was also found by Ramos and Huertas (2014) and Lackovic et al. (2003, who

Table 2 Concentration of AuNPs(+) in the supernatant of AuNPs(+)–illite sorption samples

Sample	pH	C_{Au} (mg/L)
Sorption sample	$\sim$ 4	0.30
Sorption sample	$\sim$ 9	0.00

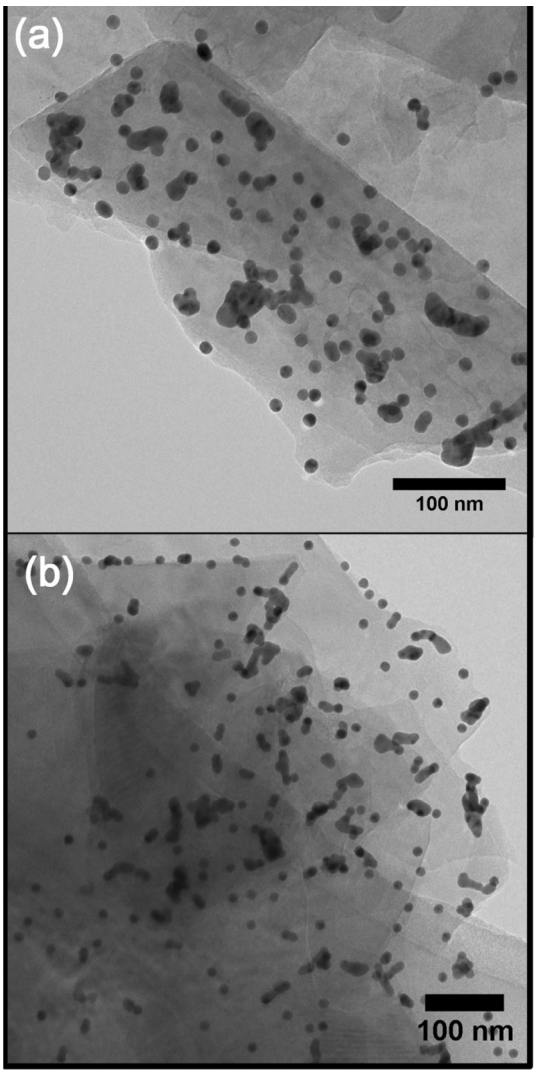

Fig. 6 TEM micrographs of the interlayer samples from AuNPs(+) sorption experiments at **a** pH ~ 4 and **b** pH ~ 9

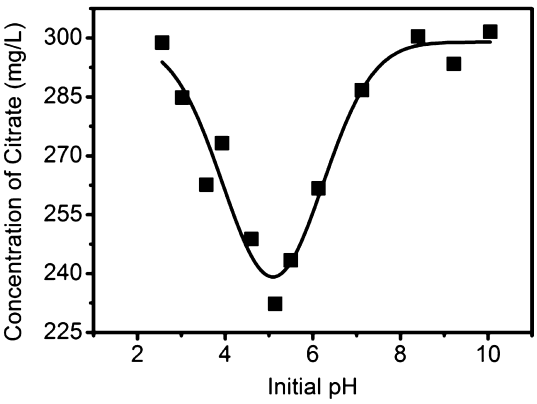

Fig. 7 Concentration of citrate after sorption as a function of pH

explained their experimental findings by surface complexation between the citrate species and clay minerals. While it is known that the electrostatic mechanism should dominate the interaction between charged citrate and illite, an obvious difference in the adsorption pattern was observed between citrate and citrate-stabilized AuNPs (Figs. 3, 7). That is, at pH < 8, the sorption quantity increased as pH declined in AuNP–illite sorption system, whereas the adsorption first increased and then decreased as pH declined in the citrate–illite sorption system.

3.3.4 Sorption mechanism

Based on the above analysis, we generalized a mechanism as a framework (as shown in Scheme 1) to explain the pH dependence of our sorption experiments. In principle, the surface charging property of illite plays a decisive role in the sorption process, which may also be modulated by the adsorption competition between free citrate molecules and AuNPs. Since citrate-capped AuNPs always carry negative charges and AuNPs(+) always carry positive charges in our whole pH range, the illite basal planes (carrying permanent negative charges) always repel the negatively charged AuNPs and adsorb the positively charged AuNPs(+) through electrostatic interactions. On the other hand, the negatively charged AuNPs can be only adsorbed on the illite edges that carry pH-dependent charges.

At pH higher than the PZC of illite (pH > 8), the illite edges carry negative charges and thus repel negatively charged citrate and AuNPs by electrostatic repulsion. At a pH value slightly lower than 8, the illite edges start to carry positive charges and can thus adsorb both citrate and AuNPs (Figs. 3, 7). However, citrate (mainly in the forms of Cit^{3-} and $HCit^{2-}$ at pH 8 to 5) may be preferentially adsorbed at the edges because of its better mobility as small molecular species compared with the much bulkier AuNPs. This effect results in the preoccupancy of the adsorbing sites by citrate at the edges and consequently inhibits the sorption of AuNPs through electrostatic repulsion (Luo et al. 2018; Wijnja and Schulthess 2000). As the pH reaches a more acidic range (from 4 to 3), although more positive charges appear at the illite edges (Scheme 1), the

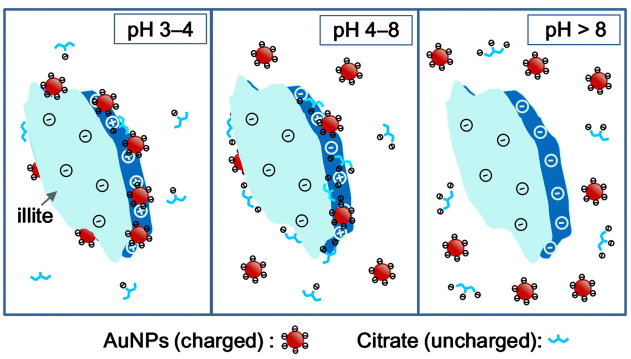

Scheme 1 Schematic presentation of the sorption mechanism

adsorption of citrate becomes weaker due to the presence of electrically neutral species (H_3Cit), which leads to dominant sorption of AuNPs.

4 Conclusions

Sorption at mineral–water interfaces may constitute a key step in many environmental processes. Our results show that electrostatic attraction was the main driving force for the sorption between illite and AuNPs, while residual citrate can also affect NP–mineral sorption through competitive adsorption. Because interactions between ENPs or NNPs and clay particles are likely in the environment, our findings will provide experimental evidence to improve our understanding of the mobility, environmental fate, and risk of NPs. Besides the often prevailing role of pH, other environmental parameters such as IS, temperature, surface organic ligands on NPs, the presence of bacteria, inorganic ions, and humic acid may also have significant influences on the interaction between minerals and NPs. Thus further study on the effects of these factors as well as the corresponding interaction mechanisms is warranted.

Acknowledgements This work was financially supported by the National Natural Science Foundation of China (41872046), Doctoral Research Startup Project in 2017 of Guizhou Normal University in China, Project of Science and Technology Supporting Plan, Guizhou Province (Qian Sci. Co.[2017], No. 2580). Besides, we thank Dr. Shirong Liu, Dr. Huayun Xiao and Dr. Baohua Xiao (Institute of Geochemistry, Chinese Academy of Sciences) for lab assistances.

Author contributions All authors contributed to the conception and design study. Data collection and analysis: YF and QW; Methodology: ZQ and SL; Writing, original draft preparation: YF; Writing, review and editing: QW, XN and WY. All authors read and approved the final manuscript.

Compliance with ethical standards

Conflict of interest The authors declare that they have no conflict of interest.

References

Avena MJ, Mariscal MM, De Pauli CP (2003) Proton binding at clay surfaces in water. Appl Clay Sci 24:3–9. https://doi.org/10.1016/j.clay.2003.07.003

Barnard AS, Guo H (2012) Nature's nanostructures. Pan Stanford Publishing Pte. Ltd., Singapore

Basu S et al (2007) Biomolecule induced nanoparticle aggregation: effect of particle size on interparticle coupling. J Colloid Interface Sci 313:724–734. https://doi.org/10.1016/j.jcis.2007.04.069

Belova V, Mohwald H, Schukin DG (2008) Sonochemical intercalation of preformed gold nanoparticles into multilayered clays. Langmuir 24:9747–9753. https://doi.org/10.1021/la8010822

Daniel MC, Astruc D (2004) Gold nanoparticles: assembly, supramolecular chemistry, quantum-size-related properties, and applications toward biology, catalysis, and nanotechnology. Chem Rev 104:293–346. https://doi.org/10.1021/cr030698+

Delhorme M, Labbez C, Caillet C, Thomas F (2010) Acid–base properties of 2:1 clays. I. Modeling the role of electrostatics. Langmuir 26:9240–9249. https://doi.org/10.1021/la100069g

Du Q, Sun ZX, Forsling W, Tang HX (1997) Acid–base properties of aqueous illite surfaces. J Colloid Interface Sci 187:221–231. https://doi.org/10.1006/jcis.1996.4631

Frens G (1973) Controlled nucleation for regulation of particle-size in monodisperse gold suspensions. Nat Phys Sci 241:20–22

Fu Y, Nie X, Qin Z, Li S, Wan Q (2017) Effect of particle size and pyrite oxidation on the sorption of gold nanoparticles on the surface of pyrite. J Nanosci Nanotechnol 17:6367–6376. https://doi.org/10.1166/jnn.2017.14417

Goswami L, Kim K-H, Deep A, Das P, Bhattacharya SS, Kumar S, Adelodun AA (2017) Engineered nano particles: nature, behavior, and effect on the environment. J Environ Manag 196:297–315. https://doi.org/10.1016/j.jenvman.2017.01.011

Gradusov BP (1974) Tentative study of clay mineral distribution in soils of world. Geoderma 12:49–55. https://doi.org/10.1016/0016-7061(74)90038-x

Gu XY, Evans LJ (2007) Modelling the adsorption of Cd(II), Cu(II), Ni(II), Pb(II), and Zn(II) onto Fithian illite. J Colloid Interface Sci 307:317–325. https://doi.org/10.1016/j.jcis.2006.11.022

Guo P, Xu N, Li D, Huangfu XX, Li ZL (2018) Aggregation and transport of rutile titanium dioxide nanoparticles with montmorillonite and diatomite in the presence of phosphate in porous sand. Chemosphere 204:327–334. https://doi.org/10.1016/j.chemosphere.2018.04.041

Gupta GS, Senapati VA, Dhawan A, Shanker R (2017) Heteroagglomeration of zinc oxide nanoparticles with clay mineral modulates the bioavailability and toxicity of nanoparticle in *Tetrahymena pyriformis*. J Colloid Interface Sci 495:9–18. https://doi.org/10.1016/j.jcis.2017.01.101

Hata H, Kobayashi Y, Salama M, Malek R, Mallouk TE (2007) pH-dependent intercalation of gold nanoparticles into a synthetic fluoromica modified with poly (allylamine). Chem Mater 19:6588–6596. https://doi.org/10.1021/cm701936y

Hong HL, Wang QY, Chang JP, Liu SR, Hu RZ (1999) Occurrence and distribution of invisible gold in the Shewushan supergene gold deposit, southeastern Hubei, China. Can Mineral 37:1525–1531

Hotze EM, Phenrat T, Lowry GV (2010) Nanoparticle aggregation: challenges to understanding transport and reactivity in the environment. J Environ Qual 39:1909–1924. https://doi.org/10.2134/jeq2009.0462

Hough RM, Noble RRP, Reich M (2011) Natural gold nanoparticles. Ore Geol Rev 42:55–61. https://doi.org/10.1016/j.oregeorev.2011.07.003

Keller AA, McFerran S, Lazareva A, Suh S (2013) Global life cycle releases of engineered nanomaterials. J Nanopart Res. https://doi.org/10.1007/s11051-013-1692-4

Kim HJ, Phenrat T, Tilton RD, Lowry GV (2012) Effect of kaolinite, silica fines and pH on transport of polymer-modified zero valent iron nano-particles in heterogeneous porous media. J Colloid Interface Sci 370:1–10. https://doi.org/10.1016/j.jcis.2011.12.059

Kraepiel AML, Keller K, Morel FMM (1998) On the acid–base chemistry of permanently charged minerals. Environ Sci Technol 32:2829–2838. https://doi.org/10.1021/es9802899

Kriaa A, Hamdi N, Srasra E (2009) Proton adsorption and acid–base properties of Tunisian illites in aqueous solution. J Struct Chem 50:273–287

Lackovic K, Johnson BB, Angove MJ, Wells JD (2003) Modeling the adsorption of citric acid onto Muloorina illite and related clay minerals. J Colloid Interface Sci 267:49–59. https://doi.org/10.1016/s0021-9797(03)00693-3

Liu JF, Legros S, Ma GB, Veinot JGC, von der Kammer F, Hofmann T (2012) Influence of surface functionalization and particle size on the aggregation kinetics of engineered nanoparticles. Chemosphere 87:918–924. https://doi.org/10.1016/j.chemosphere.2012.01.045

Liu XD, Lu XC, Sprik M, Cheng J, Meijer EJ, Wang RC (2013) Acidity of edge surface sites of montmorillonite and kaolinite. Geochim Cosmochim Acta 117:180–190. https://doi.org/10.1016/j.gca.2013.04.008

Luo S, Nie X, Yang M, Fu Y, Zeng P, Wan Q (2018) Sorption of differently charged gold nanoparticles on synthetic pyrite. Minerals 8:428. https://doi.org/10.3390/min8100428

Monfared AD, Ghazanfari MH, Kazemeini M, Jamialahmadi M, Helalizadeh A (2018) Wettability alteration modeling for oil-wet calcite/silica nanoparticle system using surface forces analysis: contribution of DLVO versus non-DLVO interactions. Ind Eng Chem Res 57:14482–14492. https://doi.org/10.1021/acs.iecr.8b01918

Nichols RJ, Burgess I, Young KL, Zamlynny V, Lipkowski J (2004) A quantitative evaluation of the adsorption of citrate on Au(111) using SNIFTIRS. J Electroanal Chem 563:33–39. https://doi.org/10.1016/j.jelechem.2003.08.007

Paek SM, Jang JU, Hwang SJ, Choy JH (2006) Exfoliation–restacking route to Au nanoparticle-clay nanohybrids. J Phys Chem Solids 67:1020–1023. https://doi.org/10.1016/j.jpcs.2006.01.021

Palenik CS, Utsunomiya S, Reich M, Kesler SE, Wang LM, Ewing RC (2004) "Invisible" gold revealed: direct imaging of gold nanoparticles in a Carlin-type deposit. Am Mineral 89:1359–1366

Park J-W, Shumaker-Parry JS (2014) Structural study of citrate layers on gold nanoparticles: role of intermolecular interactions in stabilizing nanoparticles. J Am Chem Soc 136:1907–1921. https://doi.org/10.1021/ja4097384

Peralta-Videa JR, Zhao L, Lopez-Moreno ML, de la Rosa G, Hong J, Gardea-Torresdey JL (2011) Nanomaterials and the environment: a review for the biennium 2008–2010. J Hazard Mater 186:1–15. https://doi.org/10.1016/j.jhazmat.2010.11.020

Pernodet N et al (2006) Adverse effects of citrate/gold nanoparticles on human dermal fibroblasts. Small 2:766–773. https://doi.org/10.1002/smll.200500492

Ramos ME, Huertas FJ (2014) Adsorption of lactate and citrate on montmorillonite in aqueous solutions. Appl Clay Sci 90:27–34. https://doi.org/10.1016/j.clay.2014.01.007

Rostek A, Mahl D, Epple M (2011) Chemical composition of surface-functionalized gold nanoparticles. J Nanopart Res 13:4809–4814. https://doi.org/10.1007/s11051-011-0456-2

Sau TK, Murphy CJ (2004) Room temperature, high-yield synthesis of multiple shapes of gold nanoparticles in aqueous solution. J Am Chem Soc 126:8648–8649. https://doi.org/10.1021/ja047846d

Schulthess CP, Sparks DL (1986) Backtitration technique for proton isotherm modeling of oxide surfaces. Soil Sci Soc Am J 50:1406–1411

Sharma VK, Filip J, Zboril R, Varma RS (2015) Natural inorganic nanoparticles—formation, fate, and toxicity in the environment. Chem Soc Rev 44:8410–8423. https://doi.org/10.1039/c5cs00236b

Varadwaj GBB, Parida KM (2013) Montmorillonite supported metal nanoparticles: an update on syntheses and applications. RSC Adv 3:13583–13593. https://doi.org/10.1039/c3ra40520f

Wagener P, Schwenke A, Barcikowski S (2012) How citrate ligands affect nanoparticle adsorption to microparticle supports. Langmuir 28:6132–6140. https://doi.org/10.1021/la204839m

Wagner S, Gondikas A, Neubauer E, Hofmann T, von der Kammer F (2014) Spot the difference: engineered and natural nanoparticles in the environment—release, behavior, and fate. Angew Chem Int Ed 53:12398–12419. https://doi.org/10.1002/anie.201405050

Wang J, Li YF, Huang CZ, Wu T (2008) Rapid and selective detection of cysteine based on its induced aggregates of cetyltrimethylammonium bromide capped gold nanoparticles. Anal Chim Acta 626:37–43. https://doi.org/10.1016/j.aca.2008.07.037

Wang F, Yao J, Chen H, Yi Z, Xing B (2013) Sorption of humic acid to functionalized multi-walled carbon nanotubes. Environ Pollut 180:1–6. https://doi.org/10.1016/j.envpol.2013.04.035

Wang H, Dong YN, Zhu M, Li X, Keller AA, Wang T, Li F (2015) Heteroaggregation of engineered nanoparticles and kaolin clays in aqueous environments. Water Res 80:130–138. https://doi.org/10.1016/j.watres.2015.05.023

Wiesner MR, Lowry GV, Alvarez P, Dionysiou D, Biswas P (2006) Assessing the risks of manufactured nanomaterials. Environ Sci Technol 40:4336–4345. https://doi.org/10.1021/es062726m

Wijnja H, Schulthess CP (2000) Interaction of carbonate and organic anions with sulfate and selenate adsorption on an aluminum oxide. Soil Sci Soc Am J 64:898–908

Wiwanitkit V, Sereemaspun A, Rojanathanes R (2009) Effect of gold nanoparticles on spermatozoa: the first world report. Fertil Steril 91:E7–E8. https://doi.org/10.1016/j.fertnstert.2007.08.021

Zhang Z, Li H, Zhang F, Wu Y, Guo Z, Zhou L, Li J (2014) Investigation of halide-induced aggregation of Au nanoparticles into spongelike gold. Langmuir 30(10):2648–2659. https://doi.org/10.1021/la4046447

Zhao XJ, Mai ZB, Kang XH, Zou XY (2008) Direct electrochemistry and electrocatalysis of horseradish peroxidase based on clay–chitosan–gold nanoparticle nanocomposite. Biosens Bioelectron 23:1032–1038. https://doi.org/10.1016/j.bios.2007.10.012

Zhou DX, Abdel-Fattah AI, Keller AA (2012) Clay particles destabilize engineered nanoparticles in aqueous environments. Environ Sci Technol 46:7520–7526. https://doi.org/10.1021/es3004427